# The influence of facies heterogeneity on the doublet performance in low-enthalpy geothermal sedimentary reservoirs

Crooijmans, R. A.; Willems, C. J L; Maghami Nick, H.; Bruhn, D. F.

**DOI**
10.1016/j.geothermics.2016.06.004

**Publication date**
2016

**Document Version**
Accepted author manuscript

**Published in**
Geothermics

# The influence of facies heterogeneity on the doublet performance in low-enthalpy geothermal sedimentary reservoirs

R.A. Crooijmans [a], C.J.L. Willems [a], H.M. Nick [a,b], D.F. Bruhn [a,c]

[a] *Faculty of Civil Engineering and Geosciences, Delft University of Technology, The Netherlands*

[b] *The Danish Hydrocarbon Research and Technology Centre, Technical University of Denmark*

[c] *Helmholtz Centre Potsdam - GFZ German Research Centre for Geosciences*

---

*Keywords:* non-isothermal flow, variable fluid properties, heterogeneity, geothermal, doublet, sedimentary formation, net to gross ratio.

---

*rogiercrooijmans@hotmail.com

## Abstract

A three-dimensional model is used to study the influence of facies heterogeneity on energy production under different operational conditions of low-enthalpy geothermal doublet systems. Process-based facies modelling is utilised for the Nieuwerkerk sedimentary formation in the West Netherlands Basin to construct realistic reservoir models honouring geological heterogeneity. A finite element based reservoir simulator is used to model the fluid flow and heat transfer over time. A series of simulations is carried out to examine the effects of reservoir heterogeneity (Net-to-Gross ratio, N/G) on the life time and the energy recovery rate for different discharge rates and the production temperature ($T_{min}$) above which the doublet is working. With respect to the results, we propose a design model to estimate the life time and energy recovery rate of the geothermal doublet. The life time is estimated as a function of N/G, $T_{min}$ and discharge rate, while the design model for the energy recovery rate is only a function of N/G and $T_{min}$. Both life time and recovery show a positive relation with an increasing N/G. Further our results suggest that neglecting details of process-based facies modelling may lead to significant errors in predicting the life time of low-enthalpy geothermal systems for N/G values below 70%.

## 1. Introduction

Geothermal energy production from deep geological formations has been growing in the Netherlands since the first doublets were realised in 2007(van Heekeren, 2015). The main targets are sedimentary fluvial reservoirs at depths between 2 and 2.5 km with a temperature between 70 and 90 $^{\circ}C$

(Bonté et al., 2012). These are so-called low-enthalpy reservoirs, which are mainly used for heating of buildings in the horticultural sector. The sedimentary fluvial reservoirs have different characteristics from conventional geothermal in magmatic settings. Such characteristics are, for example, porosity, initial temperature, permeability and heat capacity that lead to different geothermal performance indicators such as the life time of the doublet (how long the doublet can produce economically), recovery (produced energy compared to the total amount of available energy) and the daily energy production. The performance indicators together with the operational costs determine the profitability of the geothermal system. The focus of this study is on the performance of such a system where the life time and the recovery are dependent on both human and physical controlled parameters.

Saeid et al. (2015) suggest that the most influencing human controlled parameter is the discharge of the wells. Not surprisingly, the larger the discharge the faster the cooling of the reservoir is noticeable in the production fluid (i.e. the earlier the arrival of the cold water front). Other important human controlled parameters are injection temperature and well spacing. The larger the difference in temperature between the produced and injected fluid, the more energy is extracted from the reservoir; and the closer the wells the faster the cold water reaches the production well.

The main physical controlled parameters are porosity, salinity of the pore fluid, initial reservoir temperature (Saeid et al., 2015), reservoir thickness and the thickness of shale layers in between the reservoir bodies (Poulsen et al., 2015). The salinity of the pore fluid and the initial reservoir temperature can be assumed constant at reservoir scale. Porosity is, however, strongly heterogeneous and dependent on the facies. Facies are geological bodies formed by sedimentological processes, which are dependent on the paleo-river behaviour. This makes the distribution of the facies unique for each river deposit. The facies with high porosity and permeability form the reservoir bodies.

Within the oil industry the spatial distribution and geometry of the reservoir bodies is commonly investigated (Jones et al., 1995; Willis and Tang, 2010; Attar et al., 2015). The geometry and distribution control the reservoir connectivity, which is the ratio of the volume of the largest connected reservoir body over the sum of the volume of all reservoir bodies. The connectivity is closely linked to the net-to-gross ratio (N/G), which is the net reservoir volume versus the total volume (Hovadik and Larue, 2007). Above 50% N/G the connectivity is more than 95% and it is unlikely that this is a significant uncertainty (King, 1990). For fluvial reservoir systems the connectivity is most sensitive between 10 and 20% N/G. The connectivity is about 20% for reservoirs with N/G of 10% and it reaches 80% for reservoirs of 20% N/G (Larue and Hovadik, 2006). This range in N/G is river type dependent; for example, for rivers with high sinuosity the range shifts to lower N/G values (Hovadik and Larue, 2007).

Larue and Hovadik (2008) studied the effect of N/G and connectivity on oil recovery in a doublet system. For reservoirs with a connectivity above 95%, they found that geological parameters such as sinuosity and width/thickness ratio of the geo bodies and the orientation of the wells compared to the geobodies have a relatively small effect on recovery and water flooding efficiency. There is a small drop in oil recovery when the

N/G decreases from 50% to 20%. Below the 20% N/G the oil recovery drops drastically from 80% to roughly 25% (Larue and Hovadik, 2008).

In the geothermal sector depositional processes and the building of various sedimentological architectures are not commonly considered when the effect of human controlled and physical parameters on the doublet performance is investigated. Simplified geological representations are commonly used such as homogeneous models (Saeid et al., 2014) or layer cake models (Poulsen et al., 2015; Mottaghy et al., 2011; Deo et al., 2014). In the Netherlands the software program 'DoubletCalc' is commonly used for prediction of the doublet performance. This free software provided by TNO uses homogeneous sand box models to calculate the obtained power of a low-enthalpy geothermal doublet (Mijnlief et al., 2012), assuming that the connectivity and N/G are both 100%. Studies in the oil-sector, however, show that these parameters have a major impact on the fluid flow patterns (Hovadik and Larue, 2007) and the recovery (Larue and Friedmann, 2005; Hovadik and Larue, 2007; Larue and Hovadik, 2008). The lessons learnt in the oil industry sector provide some insight on the importance of the use of detailed reservoir representations in a geothermal system. These lessons however cannot be applied directly to geothermal studies because oil is only extracted from the pore volume, while the heat extracted from geothermal reservoirs is obtained from the fluid in the pores and from the rock matrix.

In this paper process-based facies modelling is used to create realistic representations of sedimentary reservoirs. Over 45 representations, called reservoir realisations are created with a N/G ranging from 10 to 100%. A finite element method (FEM) is utilised to simulate the fluid flow and heat transfer processes in geothermal doublets. In the first part of this paper the modelling approach is explained for both the generation of reservoir realisations and the non-isothermal simulations. Next the relation between N/G and the doublet performance parameters (life time and recovery) is discussed, followed by the effect of the discharge rate. Then, the results are combined to obtain a so-called 'design model', which estimates the life time of a doublet and the recovery. In the end the difference between randomly generated realisations and the reservoir realisations is assessed to highlight the relevance of the facies based reservoir realisation in low-enthalpy geothermal reservoir modelling.

## 2. Methodology

### *2.1. Reservoir models*

This work consists of two main parts: static geomodels and dynamic reservoir simulation. The static geomodels, with different N/G ranging from 10 to 100%, are generated in three different ways: Model Type I and II are made utilising a process-based facies modelling approach to distribute different facies Types (i.e. sand, shale); Model Type III is made using a random facies field generator. The difference between Type I and II is the way in which properties are assigned to the sand bodies. In Type I porosity and permeability are heterogeneous within the sand bodies whereas in the Model Type II single average porosity and permeability values are assigned for the sand bodies. The realisations are then employed for conducting dynamic simulations (Figure 1). The heat transfer in the reservoir and temperature at the production well are calculated over time by using the software package

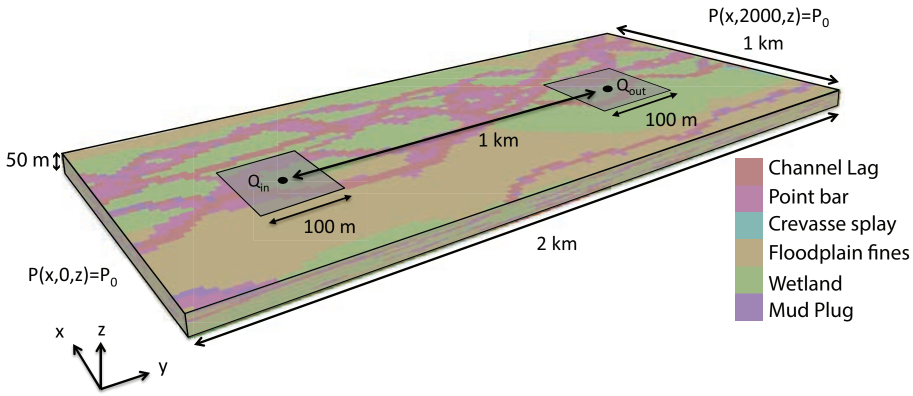


Figure 1: Schematic of the model domain and the well locations.

COMSOL Multiphysics utilising a finite element method. In the base case (initial) scenario the discharge is 100 $m^3/h$, the initial reservoir temperature is 75 °C and for the base case scenario the production stops when the production temperature drops to 74 °C (Minimal production temperature, $T_{min}$). The decline in the production temperature can be seen as the arrival time of the cold water front. Flow and heat transfer simulations are conducted employing all the generated reservoir realisations for several scenarios with different discharge rates (80, 100, 120 and 140 $m^3/h$). Consequently, the life time values and total heat recovery are calculated for different minimal production temperatures (74, 72, 70 and 68 °C).

### *2.1.1. Reservoir model Type I, II and III*

Process-based facies modelling software Flumy (Grappe et al., 2012) is utilised to generate 48 realisations (depositional models) of a 1km×2km×50m geothermal reservoir with a resolution of 20m×20m×2.5m. In this process-based approach, facies are distributed mainly by modelling sedimentological processes. Lopez et al. (2009) suggest that the constructed reservoir models utilising a combined stochastic and process-based approach are realistic. This is because the channels sizes and shapes are explicitly related to channel width, channel depth, and avulsion frequency within other controlling parameters. For example, the location of a fluvial channel after the avulsion depends on the topography created by the previous flow path and deposition of sediment. Note that while the constructed models are not conditioned by input data such as logs or cores the geological data constrains range of the controlling parameters in the process-based model. The method is explained in detail in Grappe et al. (2012) and Lopez et al. (2009).

The resulting realisations contain seven Types of geobodies; pointbars, sand plugs, channel lag, crevasse splays, levees, overbank floodplain fines and mud plugs. The sedimentological processes depend on parameters such as avulsion frequency, flood frequency, paleo-channel width and depth, maximum floodplain deposit thickness and topography of the floodplain. In all of the generated realisations the paleo flow, from the southeast to northwest is oriented parallel to the long edge of the reservoir boundary (Figure 1). The paleo-channel width and depth considered in this study are 40m and 4m, respectively. These values and paleo-flow direction are derived from core interpretations of the Lower Cretaceous Nieuwerkerk Formation in the West

Table 1: Reservoir sand body geometries.(*Donselaar and Overeem, 2008; Pranter et al., 2007**).

| | |
|---|---|
| Bank-full flow width | 40m* |
| Bank-full flow depth | 4m |
| Meander belt width | 800-1200m* |
| Single-story sandstone body thickness | 4-5m |
| Single-story sandstone body width | 200-400m* |
| Multi-story sandstone thickness | 6-20m |
| Multi-story sandstone width | 100-500 |
| Width/thickness ratio sandstone bodies | 16-100** |

Netherlands Basin (DeVault and Jeremiah, 2002). The choice of orienting the paleo-flow direction parallel to the long-edge increases the connectivity in the reservoir realisations compared to a paleo flow perpendicular to the long edge. The ranges of process parameter values used for the modelling are derived from well core data and presented in Table 1 .

After the reservoir realisations are generated, the model is simplified by dividing the 7 types of geobodies into two groups; sand (channel lag, point bar, sand plug) and shale (crevasse splay, levee, overbank alluvium, mud plug). The sand group is considered as reservoir and the shale group as non-reservoir and the groups are used to calculate the N/G of the realisations. Sandstone grain size heterogeneity within sandstone bodies depends on paleo flow speed, and the proximity to the channel axis and river bends. As a result, the permeability of channel lags, point-bars and sand plugs varies across sandstone bodies (Willis and Tang, 2010). Therefore the heterogeneity of the facies in the sand group is assumed to be captured by using the sandstone permeability distribution from the core measurements (TNO, 1977). A beta distribution correlation function was used to generate a heterogeneous porosity field within the sand group. The distribution characteristics including: mean, standard deviation, skew and kurtosis are equal to 0.28, 0.075, 0.35 and 2.3, respectively. The permeability of this group is derived from a porosity-permeability relationship obtained from petrophysical data of well MKP-11 (TNO, 1977):

$$\kappa = 0.0633 e^{29.507\phi} \tag{1}$$

Where $\kappa$ is the permeability [mD] and $\phi$ is the porosity [-]. The effect of heterogeneity in the thermal rock properties on heat transfer in the geothermal reservoir is insignificant compared to the heterogeneity in the flow properties (Mottaghy et al., 2011). Therefore the thermal rock properties are considered homogeneous and isotropic. The porosity and permeability of the shale group are also assumed to be homogeneous and isotropic (Table 2).

To determine the effect of the heterogeneous porosity of the reservoir bodies, some of the reservoir realisations are rebuilt with a homogeneous sand group and named as model Type II. The porosity and permeability of the sand group is equal to the averaged porosity and permeability of the sand group in the reservoir realisations of model Type I. The size and distribution of the reservoir bodies are kept the same.

Further, to study the relevance of process-based facies modelling on the estimation of the life time and energy production of the doublets, geo-model realisations (model Type III) are generated with the sand and shale facies randomly (uncorrelated) distributed. The reservoir bodies have a constant porosity of 28% and constant permeability of 1000 mD. All other parameters are kept constant as in the model Type I. The differences in life time and production between a processed-based facies reservoir model (Type I) and a random realisation (Type III) are a measure of the importance of process-based models used in geothermal reservoir simulations.

### *2.2. Flow and heat transfer model*

The generated reservoir realisations (Type I, II and III) are employed for heat transfer and fluid flow modelling. Figure 1 illustrates the reservoir and the well locations (well spacing is 1 km). The injection and the production wells have the same discharge rate which remains constant over time. The two outer boundaries at the short edge are assigned a constant pressure, the others are no flow boundaries (Figure 1). The N/G at the well positions, in all dynamic models, has to be roughly the same as the N/G of the field, especially for reservoir realisations with low N/G. In some of the reservoir realisations the well may not be in contact with any sand body. This would increase the well pressure and change the flow patterns within the realisation. In this work, the maximum allowable difference between N/G at the wells and the reservoir realisation is 2.5%. To achieve this the doublet can be placed within a range of 50 m in the x and y direction from the original well locations (Figure 1). The orientation of the doublet and the distance between the wells are kept constant in all simulations.

#### *2.2.1. Governing equations*

Heat transfer in geothermal systems can be described with two main processes: conduction and convection. For a system with a rigid rock, incompressible fluids and local thermal equilibrium between rock and fluid the heat transfer equation reads:

$$\frac{\partial}{\partial t}(\rho CT) = \nabla \cdot (\boldsymbol{\lambda} \nabla T) - \nabla \cdot (\rho_f C_f \mathbf{u} T) + \rho_f C_f q T^* \quad (2)$$

Where $t$ is time $[s]$, $T$ the temperature [K], $\boldsymbol{\lambda}$ the total conductivity tensor [W/(kgK)], $\rho_f$ the fluid density [kg/m$^3$], $C_f$ the fluid specific heat capacity [J/mK], $\mathbf{u}$ Darcy velocity vector [m/s], and $\rho C$ is the volumetric heat capacity, $q$ is external sinks and sources [1/s], and $T^*$ refers to the temperature at sources. Darcy velocity is calculated as: $\mathbf{u} = -(\kappa/\mu)\nabla P$. Where $\mu$ is the dynamic viscosity [Pa.s] and $P$ is the fluid pressure [Pa]. The fluid pressure field can be obtained by solving the continuity equation: $\phi \partial \rho_f / \partial t + \nabla \cdot (\rho_f \mathbf{u}) = \rho_f q$. The total thermal conductivity is expressed as: $\boldsymbol{\lambda} = \lambda_{eq} \boldsymbol{I} + \boldsymbol{\lambda}_{dis}$. Where $\lambda_{eq}$ is the equivalent conductivity of the fluid and the matrix and the $\boldsymbol{\lambda}_{dis}$ the thermal dispersion tensor. This equivalent conductivity and the volumetric heat capacity are both volume averaged:

$$\begin{aligned} \lambda_{eq} =& (1-\phi)\lambda_s + \phi \lambda_f \\ \rho C =& (1-\phi)\rho_s C_s + \phi \rho_f C_f \end{aligned} \quad (3)$$

Where the suffixes $s$ and f stand for solid (shale, sand) and fluid (brine), respectively.

Thermal dispersion has influence on the total conductivity. Thermal dispersion can be described as a function of the fluid velocity and fluid heat properties. The thermal dispersion tensor which is based on the solute dispersion model (Scheidegger, 1961), reads:

$$\boldsymbol{\lambda} = (\lambda_{eq} + (\alpha_T)|\mathbf{u}|)\mathbf{I} + \rho_f C_f\,(\alpha_L - \alpha_T)\,\frac{\mathbf{uu}}{|\mathbf{u}|} \tag{4}$$

$|\mathbf{q}|$ is the magnitude of the Darcy velocity vector and $\alpha_L$ and $\alpha_T$ are the thermal dispersion coefficients in the longitudinal and transversal direction, respectively.

The pore fluid used in the dynamic model is brine. The brine has a constant specific heat capacity, heat conductivity and salinity (Table 2). The viscosity of the brine varies with temperature ($T$) and $S$ the salinity of the brine [ppm/$10^6$] (Batzle and Wang, 1992) as:

$$\mu = 0.1 + 0.333S + (1.65 + 91.9S^3)e^{\left\{-\left[0.42\left(S^{0.8}-0.17\right)^2+0.045\right]T^{0.8}\right\}} \tag{5}$$

The density of the brine depends on the temperature, the pressure and the salinity as:

$$\begin{aligned}\rho_f =& \rho_w + S\{0.668 + 0.44S + 10^{-6}[300P - 2400PS \\ &+ T(80 + 3T - 3300S^3P + 47PS)]\}\end{aligned} \tag{6}$$

Where

$$\begin{aligned}\rho_w =& 1 + 10^{-6}(-80T - 3.3T^2 + 0.00175T^3 + 489P - 2TP + 0.016T^2P \\ &- 1.3 * 10^{-5}T^3P - 0.333P^2 - 0.002TP^2)\end{aligned} \tag{7}$$

For equations 5 to 7, $T$ is in [°C] and $P$ in [MPa] (Batzle and Wang, 1992).

The model domain is discretised by 3D tetrahedral and hexahedral finite elements. In general, discretization errors are the dominant sources of numerical errors in simulations (e.g. Nick et al., 2009). To minimise the discretisation error a maximum finite element mesh size of 20×20×2.5 m is chosen. The minimum finite element mesh size is 0.5 m. The maximum mesh size is the same as the resolution of the geomodels. This avoids porosity and permeability upscaling (averaging properties due to grid coarsening) of reservoir realisations. Saeid et al. (2015) analysed the discretisation error for a similar dynamic model and found that the chosen mesh size results in a negligible discretisation error for the fluid and heat transfer simulations for the range of studied parameters. In this study, the relative and absolute error tolerances for flow and heat transport simulations are set to $10^{-5}$ and $10^{-6}$, respectively.

#### 2.2.2. Life time

The water temperature calculated at the production well is used to obtain the life time of the doublet. The life time of the doublet is determined at the time when the production fluid temperature drops below the minimal production temperature. The temperature losses in the surface facilities and the wells are neglected. Saeid et al. (2015) illustrated that the temperature losses in the wells have negligible effect on the temperature of the production fluid of a geothermal system.

#### 2.2.3. Recovery and Net energy production

The calculated production temperature over time can be used to obtain recovery, $R = E_{prod}/E_{total}$. Where $R$ is the recovery of the field [%], $E_{prod}$ the cumulative produced energy [J] and $E_{total}$ the total available energy [J]. The cumulative produced energy is defined as:

$$E_{prod} = \sum_{i=1}^{n} Q_i \Delta t_i \rho_f C_f \left(T_{prod,i} - T_{inj}\right), \qquad (8)$$

and the total available energy as:

$$E_{total} = \sum_{j=1}^{m} \quad \{V_j \phi_j \rho_{f,j} C_{f,j} \left(T_0 - T_{inj}\right) + V_j (1 - \phi_j) \rho_{s,j} C_{s,j} \left(T_0 - T_{inj}\right)\} \qquad (9)$$

Where $\Delta t$ is the time step increment, the subscript i the time step, n total number of time steps, Q the discharge [m$^3$/s], $T_{prod,i}$ and $T_{inj}$ the temperature [K] of the production fluid and the injection fluid at step i, respectively. $m$ is the total number of finite elements, $V_j$ the volume of the mesh element j and $T_0$ is the initial temperature [K].

The energy production is the produced energy minus the pump energy that is required to induce a pressure difference between the injection and the production well: $E_{net} = E_{prod} - E_{pump}$. Where $E_{pump}$ is the required pump energy, assuming the efficiency of the pumps is equal to 1:

$$E_{pump} = \sum_{i=1}^{n} Q \Delta t_i (P_{inj} - P_{prod}) \qquad (10)$$

## 3. Results

### *3.1. Base case*

When applying the base case conditions for the dynamic simulation of different realisations of model Type I the following features were observed: (i) the N/G has noticeable impact on the life time of the doublet especially

Table 2: List of parameters used in the dynamic model.

| Parameter | Description | Value | Dimension |
|---|---|---|---|
| $\alpha_L$ | Longitudinal dispersion coefficient | 6.5 | m |
| $\alpha_T$ | Transversal dispersion coefficient | 2.2 | m |
| $\kappa_{shale}$ | Permeability of the shale bodies | 5 | mD |
| $\lambda_f$ | Conductivity of the pore fluid | 0.7 | W/m/K |
| $\lambda_{sand}$ | Conductivity of the sand bodies | 2.7 | W/m/K |
| $\lambda_{shale}$ | Conductivity of the shale bodies | 2.0 | W/m/K |
| $\rho_{sand}$ | Density of the sand bodies | 2650 | $kg/m^3$ |
| $\rho_{shale}$ | Density of the shale bodies | 2600 | $kg/m^3$ |
| $\phi_{sand}$ | Average porosity of the sand bodies | 0.28 | - |
| $\phi_{shale}$ | Porosity of the shale bodies | 0.1 | - |
| $C_f$ | Specific heat capacity of the pore fluid | 4200 | J/kg/K |
| $C_{sand}$ | Specific heat capacity of the sand bodies | 730 | J/kg/K |
| $C_{shale}$ | Specific heat capacity of the shale bodies | 950 | J/kg/K |
| $L$ | Well spacing | 1000 | m |
| $P_0$ | Initial pressure | 200 | bar |
| $S$ | Salinity of the pore fluid | 3 | $ppm/10^6$ |
| $T_0$ | Initial temperature | 348 | K |
| $T_{inj}$ | Injection temperature | 308 | K |

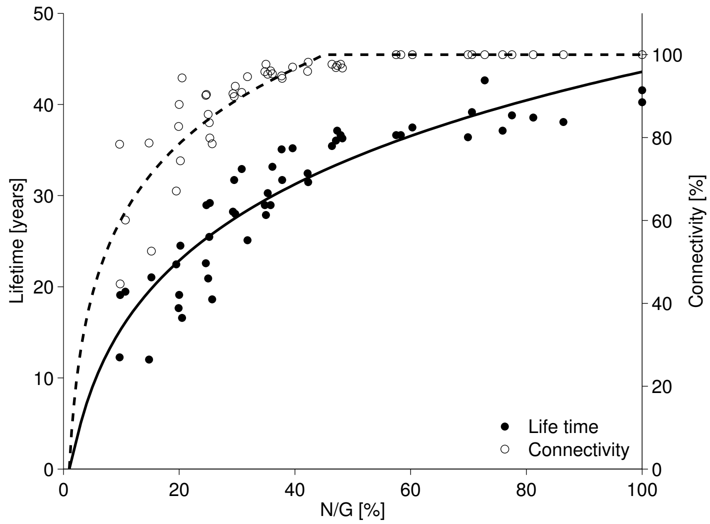


Figure 2: Life time of the doublet for $Q = 100$ m$^3$/h and $T_{min} = 74$°C and connectivity versus N/G, for model Type I realisations.

for low N/G values (Figure 2); (ii) decreasing N/G results in decreasing the life time, which is more pronounced for realisations with N/G smaller than 40%; and (iii) the cumulative energy production shows the same results as the recovery (Figure 3), but the recovery increases slightly faster at N/G values larger than 60%. Since the differences between recovery and the cumulative energy production are negligible only the obtained recovery is discussed in this study. The recovery shows a similar relation with N/G as the life time (Figure 3). Note that 40% N/G is the point where the connectivity starts to decrease with lower N/G values.

Based on the obtained life time and recovery values for the base case scenario, the life time and recovery can be described as functions of N/G:

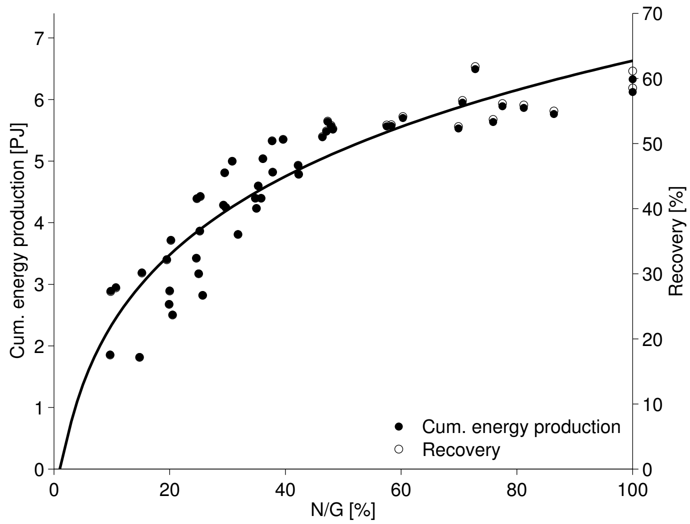


Figure 3: Total energy production and recovery versus N/G for $Q = 100$ m$^3$/h and $T_{min} = 74$°C utilising model Type I realisations.

$$LT = \alpha_{LT}\ln(N/G)^{\gamma} \tag{11}$$

and

$$R = \beta_{R}\ln(N/G)^{\gamma} \tag{12}$$

Where LT is the life time [years] and R the recovery [%]. $\alpha_{LT}$ and $\alpha_R$ are the fitting parameters for life time and recovery, respectively. For the base case scenario the fitting parameters $\alpha_{LT}$, $\beta_R$ and $\gamma$ are equal to 4.41, 6.35 and 1.5, respectively.

The variation in the temperature breakthrough curves obtained at the well production for reservoir realisations (Type I) with similar N/G values increase significantly with a decreasing N/G. For a N/G of around 50% the breakthrough temperatures are almost identical (Figure 4-C). At a N/G of around 30% the time at which the temperature starts to drop and the gradient at which it drops start to differ among the realisations (Figure 4-B). The differences are even larger at a N/G around 10% (Figure 4-A). The variations can also be seen in the required energy for the pump (Figure 5). A higher energy requirement means that more energy is needed to have the same discharge implying that the sand bodies at the injection well are less connected to the sand bodies at the production well. As a result the net energy produced is less scattered than the total energy produced at very low N/G.

The difference in the temperature breakthrough curves originates from the difference in the corresponding medium configurations. Reservoir realisations with a N/G of 10% in Figure 4-A illustrate that the location and geometry of the sand bodies determine which part of the reservoir has a high permeability zone. These geometries differ per realisation. Some sand bodies go straight, while others are curved and/or split in two, which also results in isolated sand bodies in different locations in the domain. When the N/G increases this effect becomes less. At a N/G around 30% there are still some continuous shale bodies separating the sands (Figure 4-B). The shales form low permeable zones functioning as flow barriers. For realisations around 50% N/G, the sand bodies are all connected to each other and cover the whole area, which makes the realisations look more alike (Figure 4-C).

### *3.2. Effect of discharge on geothermal doublet performance*

As expected, with increased discharge rates, the life time of the doublet decreases (Figure 6). Similarly, with increased discharge, the variance in

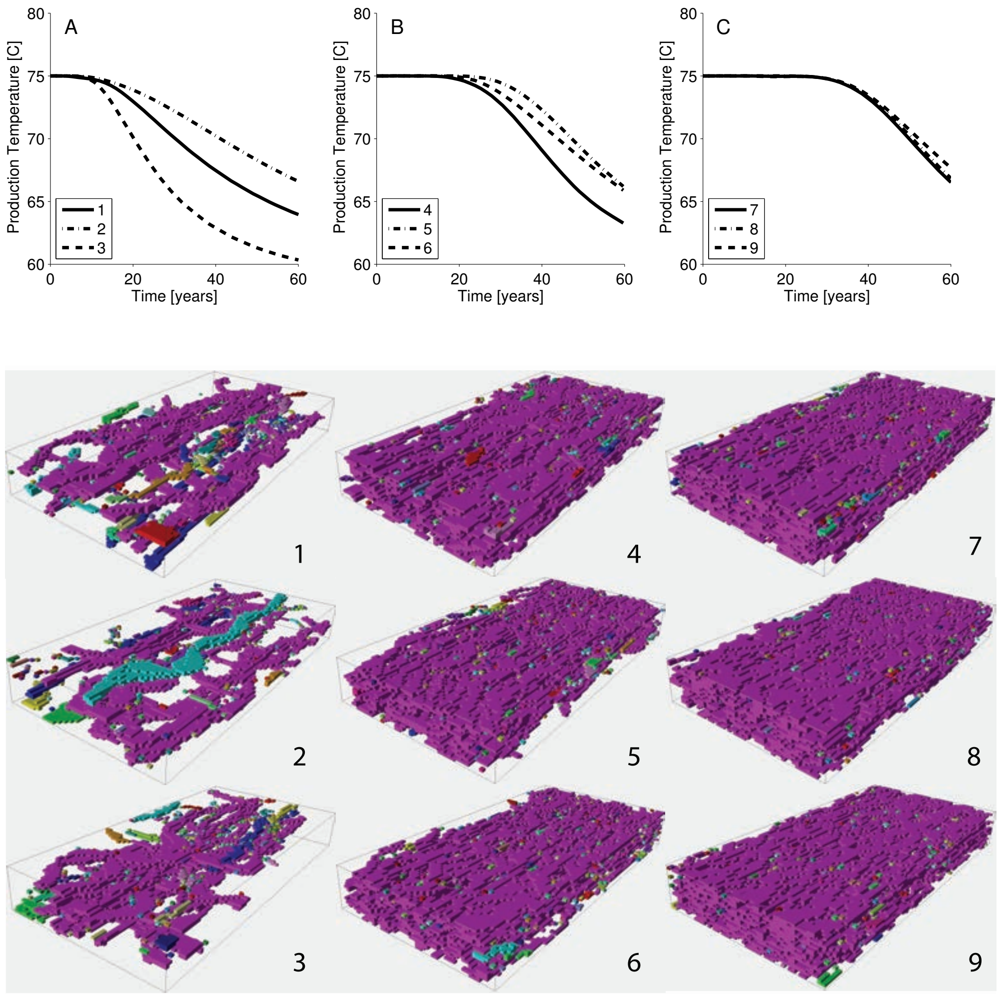


Figure 4: Production temperature development for $Q = 100$ m$^3$/h, corresponding to different Type I realisations (1 to 9). Claystone gridblocks are transparent, and connected sandstone bodies have the same colour.

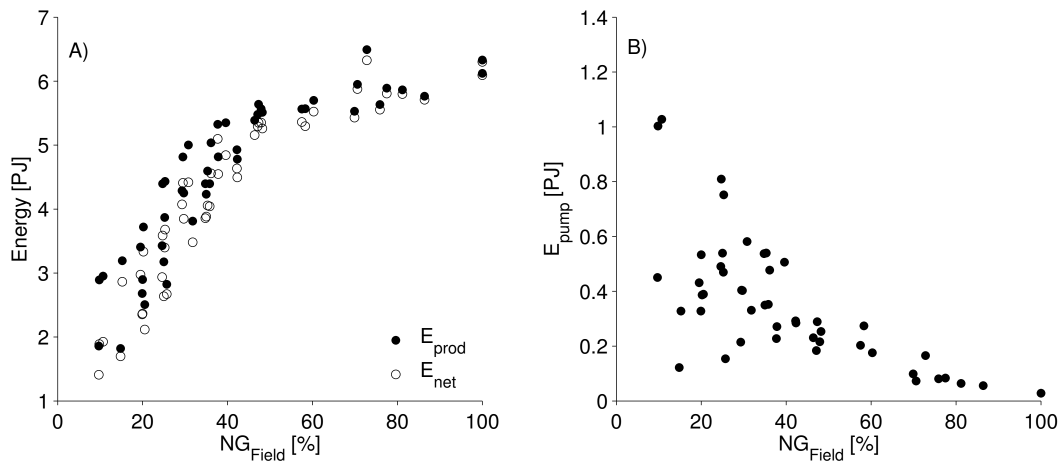


Figure 5: A) The produced energy and the net produced energy versus N/G. B) Pump energy required to create the pressure difference at the wells versus N/G (Eq. 10).

life time among realisations (Type I) is reduced (Figure 7). This is related to the fast decrease in life time for reservoirs with a large N/G. When the discharge rate goes from 60 to 100 m$^3$/h, the life time decreases with $\sim$20 years for Type I realisations with a N/G of 100%, while at a N/G of 10% life time decreases with $\sim$10 years. At high discharge rates ($Q > 200$ m$^3$/h) an increase in the discharge has rather negliglible effect on the life time, while at low discharge rates ($Q = 60$ m$^3$/h) small changes have a large impact on the life time, 10 years difference compared with $Q = 80$ m$^3$/h (Figure 7).

The type of relation between the N/G and life time does not change for different discharges, but it affects the fitting parameter $\alpha_{LT}$. This fitting parameter has a linear relation with $1/Q$ (Figure 8-A):

$$\alpha_{LT} = \frac{\alpha_Q}{Q} \tag{13}$$

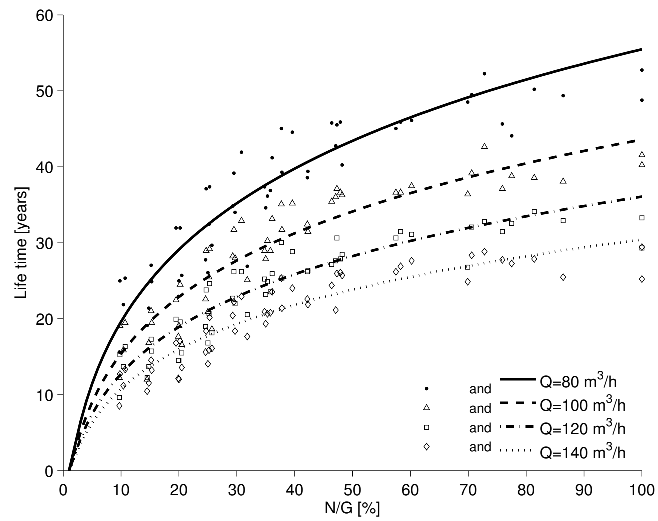


Figure 6: Life time versus N/G for different discharge rates ($T_{min} = 74°\mathrm{C}$).

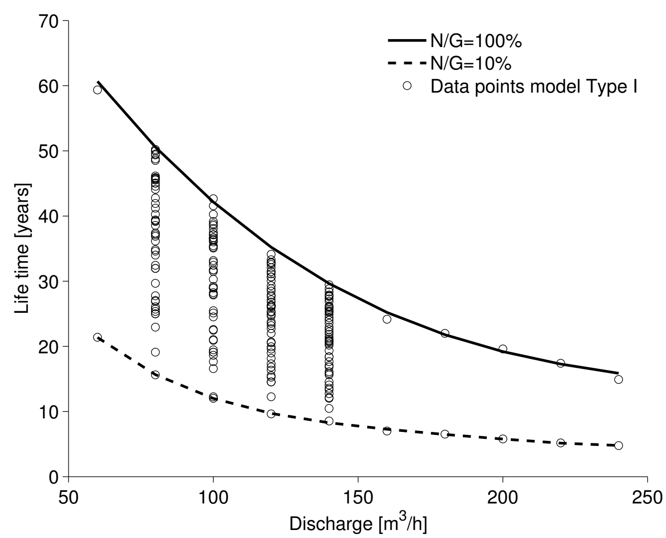


Figure 7: The variance in obtained life time values for N/G at different discharge rates and $T_{min} = 74°\mathrm{C}$

$$\beta_R = \frac{\beta_Q}{Q} \approx \text{constant} \tag{14}$$

Where $\alpha_Q$ is the discharge fitting parameter. The fitting parameter of the recovery, $\beta_R$, is barely sensitive to increasing $1/Q$ (Figure 8-B) and therefore the effect of discharge on $\beta_R$ is neglected. Neither does the discharge variation have effect on the fitting parameter $\gamma$.

### *3.3. Influence of the minimal production temperature on geothermal doublet life time and recovery*

A decrease in the minimal production temperature results in a longer life time and higher recovery (Figure 9). As a result the fitting parameters $\alpha_Q$ and $\beta_R$ are specific for each production temperature. The lower the minimal production temperature the steeper the relation between parameters $\alpha_{LT}$ and $1/Q$ (Figure 8-C). The discharge fitting parameter $\alpha_Q$ has a linear relation with the temperature difference (Figure 8-A). As a result the complete curve for life time estimations becomes steeper, which gives an overestimation for reservoirs with a N/G above 60%. To correct for this overestimation the fitting parameters $\gamma$ is defined as a function of $\Delta T$:

$$\alpha_Q = 221\Delta T + 176 \tag{15}$$

$$\beta_R = 3.04\Delta T + 2.77 \tag{16}$$

$$\gamma = -0.115\Delta T + 1.585 \tag{17}$$

where $\Delta T = T_0 - T_{prod}$. Note that this relation is best suitable for $\Delta T$ up to 10 °C.

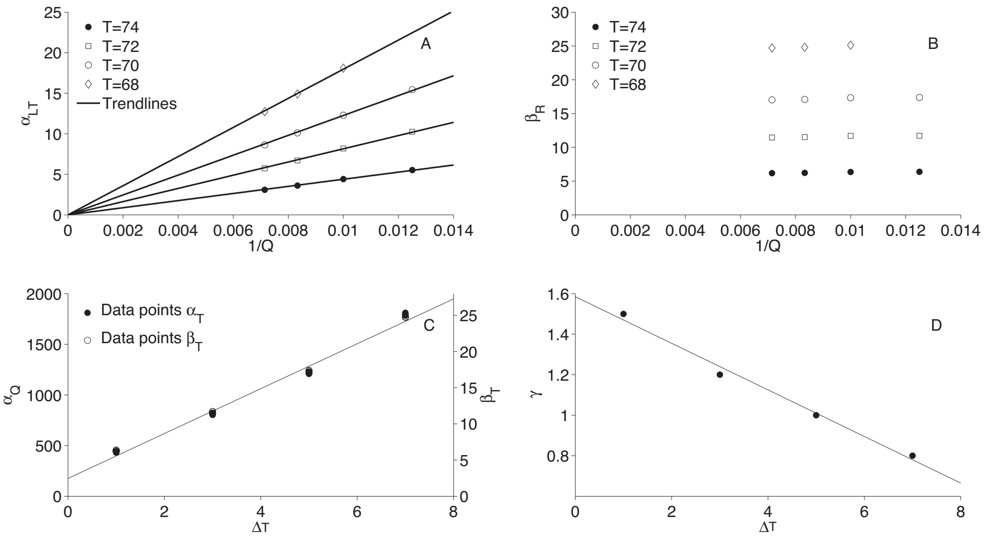


Figure 8: (A) $\alpha_{LT}$ versus $1/Q$ for different minimal production temperatures, (B) $\beta_R$ versus $1/Q$ for different minimal production temperatures, (C) $\alpha_Q$ and $\beta_T$ versus $\Delta T$ and (D) $\gamma$ versus 1/Q.

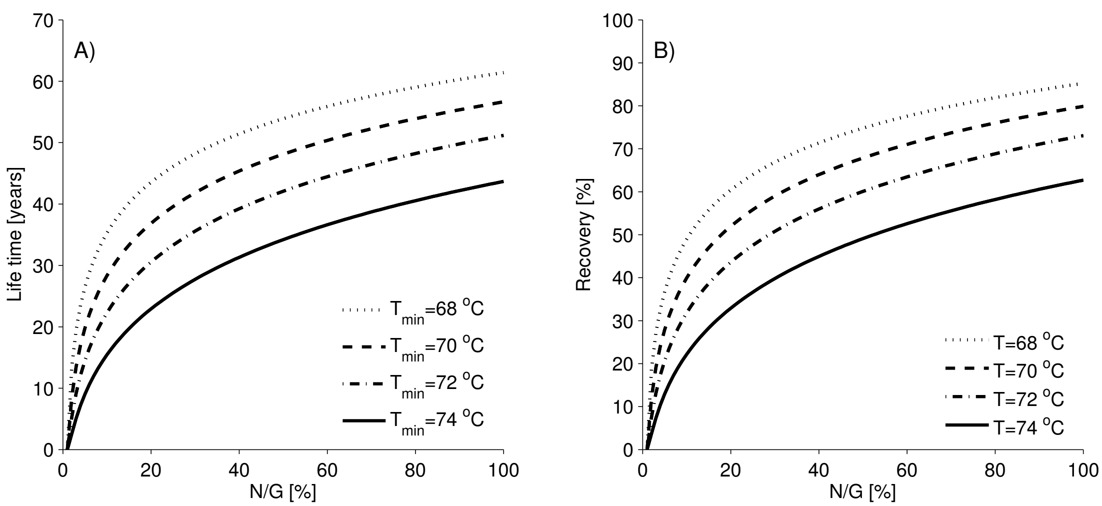


Figure 9: (A)The life time and (B) recovery versus N/G of model Type I realisations with a minimal production temperature of 68, 70, 72 and 74 °C for $Q = 100$ m$^3$/h.

### 3.4. Homogeneous versus heterogeneous reservoir bodies

The reservoir realisations with homogeneous reservoir bodies (Type II) have a slightly higher life time, 1.6 years on average with a maximum of 4.2 years, than that of model Type I realisations with heterogeneous reservoir bodies (Figure 10). The overestimation falls mostly within the uncertainty level of the calculated life times, which is related to the reservoir heterogeneity.

### 3.5. Random realisations versus Reservoir realisations

Utilising the random realisations (Type III) with N/G higher than 70% results in life time values comparable to those calculated for the model Type I realisations (Figure 11-A). Utilising model Type III realisations in the dynamic model results in an overestimation of the life time for N/G values between 70% to 40%, where the life time is almost stable. Below 40% N/G the life time starts to drop in case of Type III realisations, but less than that of the Type I realisations. It is found that the connectivity values of the reservoir for Type III realisations drops drastically and reaches zero for Type III realisations with N/G less then 30%, while the Type I realisations have a minimum connectivity of 42% (Figure 11-B). This means that the random realisations (Type III) have reservoir bodies at the wells which are small and isolated. These realisations do not have a high permeable zone between the wells. And with respect to the boundary conditions, fixed discharge, the pressure difference between the injector and producer increases significantly. The models with the random realisations (Type III) result in a much lower variance in life time for reservoirs with the same N/G value when they are compared to the life time values obtained for the model Type I realisations (Figure 11).

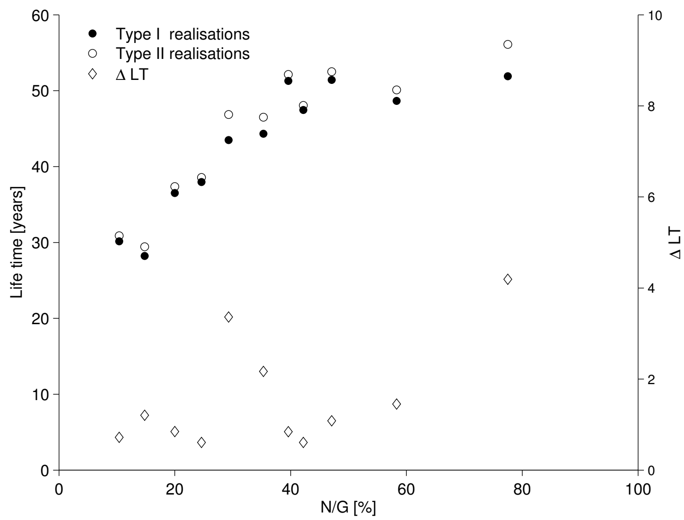


Figure 10: Life time versus N/G for reservoir realisations with heterogeneous (Type I) and homogeneous(Type II) sand bodies including the difference in life time between them(Δ LT) with $Q = 100$ m$^3$/h and $T_{min} = 74°$C.

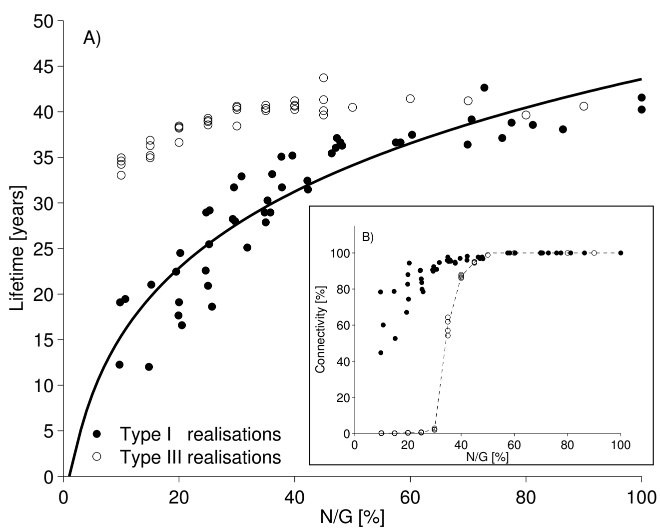


Figure 11: Life time versus the N/G of random realisation (Type III) and geological realisation (Type I) with $Q = 100$ m$^3$/h and $T_{min} = 74°$C.

### *3.6. A simple design model*

With respect to the results gained by employing the reservoir realisations Type I, the life time of a reservoir can be estimated with a simplified model when the N/G, discharge and minimal production temperature are known. The model is described as:

$$LT = \frac{221\Delta T + 176}{Q}(\ln(N/G))^{(-0.115\Delta T + 1.585)} \quad (18)$$

$$R = (3.04\Delta T + 2.77)(\ln(N/G))^{(-0.115\Delta T + 1.585)} \quad (19)$$

The model is only tested for discharge rates between 80 and 140 $m^3/h$ and minimal production temperature values down to 68 °C. More research needs to be done to check if the model is valid for higher discharge values. The linear relation of $\Delta T$ and life time is found not to be valid for all temperature values. This is because below 65 °C the production temperature curve is no longer linear (Figure 4), which indicates that the effect of $\Delta T$ on the life time is non-linear.

The results obtained with the simplified model are comparable with the results calculated with the dynamic model (Figure 12). The predicted life time values are not exactly the same as those obtained from the dynamic model. This is partly a result of the variance in life time of reservoir models with similar N/G values (Figure 11). The effect is found to be the same for the recovery.

### *3.7. An improved design model*

The simplified model works fine, but it underestimates the life time for discharges of 80 and 100 $m^3/h$ with a minimal temperature of 74°C. The

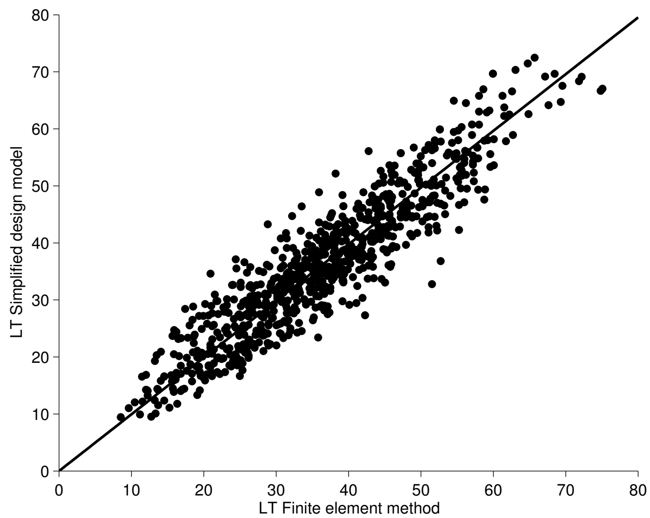


Figure 12: The life time calculated with the dynamic model versus the life time estimated with the simplified design model ($R^2 = 0.85$). The data points of all heat transfer and flow simulations of Type I are used.

model also overestimates the life time for reservoir realisation with a N/G above 70% with a minimal production temperature of 70 and 68°C. This can be improved by splitting the model up into 2 regions. Region 1 has a N/G range from 10 to 45% and Region 2 from 45 to 100% N/G. In Region 1 a similar function is used as in the simplified model, but fitting parameters are adjusted to this region (Figure 13). The function is less complex, because the fitting parameter $\gamma$ is constant. In Region 2 the function is no longer logarithmic, but linear. The improved design model is described as:

$$LT = \begin{cases} \frac{390+56.9\Delta T}{Q}(\ln(N/G))^{1.5} & \text{for } 15 < N/G \leq 45 \\ \frac{390+56.9\Delta T}{Q}(\ln(45))^{1.5} + \frac{18.7-2.84\Delta T}{Q}(N/G-45) & \text{for } 45 < N/G < 100 \end{cases} \tag{20}$$

$$R = \begin{cases} (0.75\Delta T + 5.67)(\ln(N/G))^{1.5} & \text{for } 15 < N/G \leq 45 \\ \\ (0.75\Delta T + 5.67)(\ln(45))^{1.5} & \\ +(0.28-0.035\Delta T)(N/G-45) & \text{for } 45 < N/G < 100 \end{cases} \tag{21}$$

This model describes the life time as a function of N/G, $Q$ and $\Delta T$, and the recovery as a function of only N/G and $\Delta T$. A clear distinction can be made between the two regions. In Region 1 the geological parameter N/G is the main controlling factor on both life time and recovery. The human controlled parameter $Q$ (discharge rate) is the most influential factor in Region 2 on life time, while the human controlled parameter $\Delta T$ is the most influential factor on the recovery.

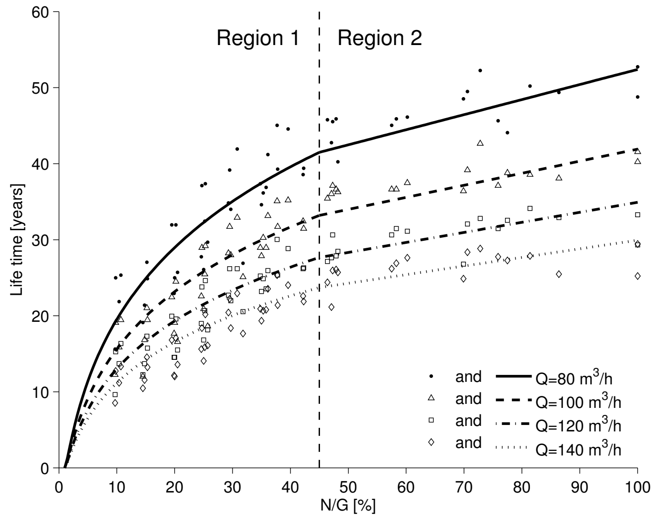


Figure 13: Life time versus N/G for different discharges based on the improved design model.

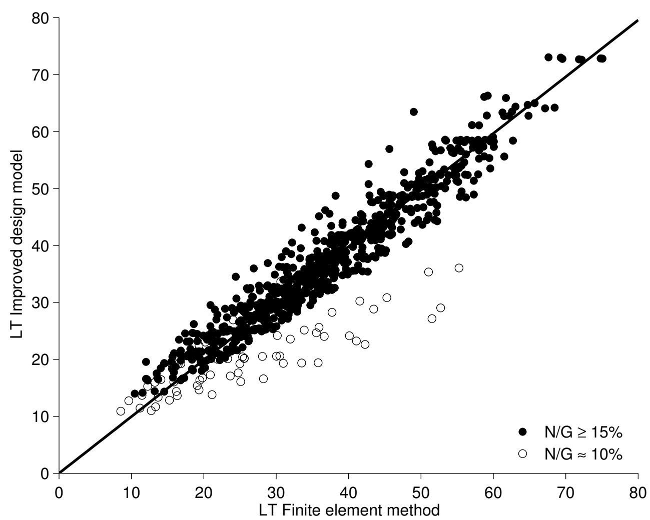


Figure 14: Life time obtained with the dynamic model versus the life time obtained with the improved design model ($R^2 = 0.92$). The data points of all heat transfer and flow simulations of Type I are used.

The improved design model predicts the life time more accurately compared to the simplified design model; it improves $R^2$ from 0.85 to 0.92 (Figures 12 and 14). The improved design model works best for N/G from 15 to 100%, but underestimates the life time of reservoirs with a N/G around 10% (Figure 14).

## 4. Discussion

### *4.1. Base case - model Type I*

The effect of N/G on life time and recovery can be described with natural logarithmic relations for N/G values below 45% and with linear relations for N/G values above 45%. In Region 1 the connectivity has a larger variance, precluding accurate prediction of the life time and recovery. The variance in connectivity increases with decreasing N/G. This could partly be an effect of the chosen resolution of the reservoir realisations (Type I), which result in less accurate connectivity calculations for a N/G below 20%. Hovadik and Larue (2007) showed that increasing the geomodel resolution decreases variance for connectivity and improves connectivity. This in combination with the effect of the facies distribution explains why it is harder to predict doublet performances of low N/G reservoirs; more variables play a role. For the linear part the relations are more accurate. The connectivity is 100% for all realisations and has therefore negligible effect on the results.

The higher variance in life time for low N/G reservoirs indicates that the accuracy of the reservoir model is crucial, which is for high N/G reservoirs with lower variances less important, albeit not negligible. The energy recovery shows the same effect as in the oil recovery; once the connectivity starts to drop the recovery drops fast (Larue and Hovadik, 2008). The absolute values of the recoveries from oil and geothermal energy can not be compared directly, because the recoveries are defined in a different way. In the oil industry the total amount of oil available is only in the pore of the reservoir bodies, while the total amount of heat available is in the connected pores and the matrix of both the reservoir and non-reservoir. This means the oil can only be produced from the reservoir part, while heat can be produced from the surrounding low permeable layers by conduction. Nonetheless, the heat recoveries obtained in this study have a range from 15 to 65% (Figure 3), which is similar to the oil recoveries reported by Larue and Hovadik (2008). The differences between obtained energy recoveries for realisations with 50 and 100% N/G are small, which indicates that the shales play an important role in geothermal doublet performance for reservoirs with N/G lower than 50%. As a result, reservoirs with a N/G of roughly 50% are almost as efficient as those with 100% N/G. Notice that the heat capacity and conductivity are similar for sand and shale, which makes the differences in heat conduction small.

#### *4.1.1. Case A: Discharge*

Discharge affects the life time and recovery, but the difference in recovery between a discharge of 80 and 140 $m^3/h$ is small compared to the variance in recovery for reservoir simulations with similar N/G (Figure 3). This means the discharge rate can be adjusted to the yearly energy demand, without influencing the cumulative produced energy significantly during the life time of the doublet.

The pressure in the injection well increases with increasing discharge or when the well is only in contact with small isolated sand bodies. This pressure can not be higher than the rock strength, otherwise the reservoir will be fractured. Fractures in the reservoir would change the fluid flow behaviour significantly (e.g. Matthäi et al., 2010; Nick et al., 2011) and the stated relations would not be applicable.

#### *4.1.2. Case B: Minimal production temperature*

Lower minimal production temperatures extend the life time and recovery. When the produced temperature declines the daily energy produced declines as well, because the discharge is constant. If a constant daily energy production is preferred the discharge has to increase to compensate for the produced water with lower temperatures. This will decrease the life time of the project and speed up the cooling of the production temperature. This loop will accelerate the whole process and the differences in life time will be less than shown in Figure 9-A.

The variance in the obtained life time and recovery increases for decreasing minimal production temperatures (Figure 4). This is related to the dispersion effect. The result of this effect is most noticeable after the cold water front has reached the production well. The temperature of the produced water drops more slowly for a system with higher thermal dispersion. This uncertainty in temperature drop makes it harder to predict the life time and recovery for lower minimal production temperatures.

### *4.2. Homogeneous sand bodies - model Type II*

Reservoir realisations with homogeneous reservoir bodies may overestimate the life time up to 4 years compared to reservoir realisations (Type I) with heterogeneous sands, but in most cases the overestimation is less than 1 year. The difference in life time between homogeneous and heterogeneous sands is within their uncertainty bounds. Therefore the intra sand-body heterogeneity could be disregarded for the life time calculation.

### *4.3. Random realisations - model Type III*

The simulations with the random realisation result in unrealistic required (well) pressure values and in much higher life times compared to reservoir realisations (Type I) when N/G values are below 70%. These unrealistic pressure values are related to the fixed discharge rate and the shape and connectivity of the reservoir bodies. Random porosity and permeability fields hardly any random realisation has a connected reservoir body from the injection to the production well, whereas the reservoir realisations do have this. As a result very high injection well pressure values are needed to push the water through the shale in between the sands in order to achieve the required discharge rate.

A realistic geological model is therefore necessary for N/G values below 40%. Above 40% N/G the connectivity plays only a small role, as it is always larger than 95%. The life time values obtained with the random realisations are overestimated for a N/G between 40 and 60%. For N/G values above 70%, the life time obtained by the random realisations are comparable with the ones obtained with reservoir realisations. Nevertheless, in the random realisations the difference between maximum and minimum possible life times is maximum 5 years, while the results of the reservoir realisation show that the difference can be significantly larger (±10 years), which seems to be the case even for reservoirs up to 70% N/G (Figure 11-A). Therefore dynamic reservoir simulations should be employed to calculate the risks of an early cold water breakthrough, especially before drilling.

Even though it is hard to make very accurate reservoir simulations before drilling, simulation results will provide a valuable range of expected life times. This means that the geology has a major impact on life time and is as important as the human controlled parameter ‘discharge’ when estimating the life time of a low-enthalpy geothermal doublet.

When layer cake models are used to calculate the life time one major assumption is that all the reservoir bodies are concentrated (i.e. 100% connectivity). The comparison of the random realisations with reservoir realisations shows that it is important to know the connectivity of the reservoir body between the injection and production well, not only for the life time, but for well pressure too. This means that if the injector is poorly connected to the producer, higher pressures are needed to keep up the discharge. This pressure varies the most for realisation below 45% N/G, which is the region where the connectivity varies (Figure 2). The pressure increases are probably less noticeable when layer cake models are used.

### *4.4. Simplified and Improved design model*

The simplified model provides a good estimate of the life time of doublets producing from low-enthalpy geothermal reservoirs. The model is only directly applicable for reservoir with roughly the same heat transfer and flow characteristics, well spacing and reservoir thickness as used in this study. The model assumes that all reservoirs have the same type of non-linear relation, but the fitting parameters are formation specific. Despite the limitations, the simplified design model can be used for primary calculations for estimating life time and recovery. It must be kept in mind, however, that the results underestimate reality for the lower range of N/G between 35 and 50% and overestimate it for a N/G above 90% (Figure 2). For the other values of N/G, the simplified model gives a good average value, when the variance in life time and recovery are taken into account.

The improved model estimates the life time more accurate than the simplified model by dividing the model into 2 regions: a logarithmic part and a linear part. This resolves the problem for the underestimations and overestimations of the simplified model and removes the fitting parameter $\gamma$ from the equation. The decreasing accuracy of the simplified model due to an increasing variance in life time remains the same in the improved model. The variance combined with an underestimation at a N/G of 10% makes the improved model less accurate for reservoirs with a N/G below 15%. This is, however, no problem for the targets for low-enthalpy geothermal reservoirs in the Netherlands, since the Nieuwerkerk Formation has a N/G between 20 and 50% (Den Hartog Jager, 1996). When applying the improved model to this formation the calculated life time can still be between 21 years (N/G=20%) and 31 years (N/G=31%) for $Q$ equal to 100 $m^3$/hr and $\Delta T$ equal to 1°C. Inclusion of N/G values measured in nearby fields in the study area can help narrowing this range of N/G and improving the life time prediction. Nevertheless this implies that accurate field data and reservoir realisations are necessary for accurate prediction of the doublets life time and recovery.

## 5. Conclusions

The work combines a process-based model with a flow and heat transfer model. The process-based model is capable of generating reservoir models (Type I and II) utilising core data. We show that the life time can be estimated with the design model for both Region 1 (N/G$>$ 45%) and Region 2 (N/G$<$ 45%). We have demonstrated that the difference in life time within Region 2 is relatively small and the main controlling factor is the discharge. In Region 1 the dependence of life time on N/G is larger than in Region 2. Therefore small over- and underestimation in N/G have a large impact on life time predictions in Region 1. The shale has a positive contribution to the heat transfer in the system, which increases the potential of lower N/G reservoirs.

When using a geological model with randomly distributed facies, first the life times are overestimated, especially for reservoirs in Region 1. Next, the variance in life time for reservoirs with the same N/G is less than 5 years for model Type III reservoirs, while it is 10 years when process-based facies modelling (Type I) is used. This means a realistic representation of the facies heterogeneity is needed to make more reliable predictions of the life time of a low-enthalpy geothermal doublet.

# References

# References

Attar, A., Muggeridge, A., et al. (2015). Impact of geological heterogeneity on performance of secondary and tertiary low salinity water injection. In *SPE Middle East Oil & Gas Show and Conference*. Society of Petroleum Engineers.

Batzle, M. and Wang, Z. (1992). Seismic properties of pore fluids. *Geophysics*, 57(11):1396–1408.

Bonté, D., Van Wees, J.-D., and Verweij, J. (2012). Subsurface temperature of the onshore netherlands: new temperature dataset and modelling. *Netherlands Journal of Geosciences*, 91(04):491–515.

Den Hartog Jager, D. (1996). Fluviomarine sequences in the lower cretaceous of the west netherlands basin: correlation and seismic expression. In *Geology of gas and oil under the Netherlands*, pages 229–241. Springer.

Deo, M., Roehner, R., Allis, R., and Moore, J. (2014). Modeling of geothermal energy production from stratigraphic reservoirs in the great basin. *Geothermics*, 51:38–45.

DeVault, B. and Jeremiah, J. (2002). Tectonostratigraphy of the nieuwerkerk formation (delfland subgroup), west netherlands basin. *AAPG bulletin*, 86(10).

Donselaar, M. E. and Overeem, I. (2008). Connectivity of fluvial point-bar deposits: An example from the miocene huesca fluvial fan, ebro basin, spain. *AAPG bulletin*, 92(9):1109–1129.

Grappe, B., Cojan, I., Flipo, N., Riviorard, J., and Vilmin, L. (2012). Developments in dynamic modelling of meandering fluvial systems. *AAPG Congres*.

Hovadik, J. M. and Larue, D. K. (2007). Static characterizations of reservoirs: refining the concepts of connectivity and continuity. *Petroleum Geoscience*, 13(3):195–211.

Jones, A., Doyle, J., Jacobsen, T., and Kjønsvik, D. (1995). Which sub-seismic heterogeneities influence waterflood performance? a case study of a low net-to-gross fluvial reservoir. *Geological Society, London, Special Publications*, 84(1):5–18.

King, P. (1990). The connectivity and conductivity if overlapping sand bodies. *North Sea Oil and Gas Reservoirs*, 2:353–362.

Larue, D. and Friedmann, F. (2005). The controversy concerning stratigraphic architecture of channelized reservoirs and recovery by waterflooding. *Petroleum Geoscience*, 11(2):131–146.

Larue, D. and Hovadik, J. (2008). Why is reservoir architecture an insignificant uncertainty in many appraisal and development studies of clastic channelized reservoirs? *Journal of Petroleum Geology*, 31(4):337–366.

Larue, D. K. and Hovadik, J. (2006). Connectivity of channelized reservoirs: a modelling approach. *Petroleum Geoscience*, 12(4):291–308.

Lopez, S., Cojan, I., Rivoirard, J., and Galli, A. (2009). Process-based stochastic modelling: meandering channelized reservoirs. *Analogue Numer Model Sediment Syst: From Understand Predict (Special Publ. 40 of the IAS)*, 40.

Matthäi, S. K., Nick, H. M., Pain, C., and Neuweiler, I. (2010). Simulation of solute transport through fractured rock: a higher-order accurate finite-element finite-volume method permitting large time steps. *Transport in porous media*, 83(2):289–318.

Mijnlief, H., Obdam, A., Kronimus, A., van Wees, J., van Hooff, P., Pluymaekers, M., and Veldkamp, J. (2012). *Doubletcalc 1.4 Handleiding.* TNO, 1.4 edition.

Mottaghy, D., Pechnig, R., and Vogt, C. (2011). The geothermal project den haag: 3d numerical models for temperature prediction and reservoir simulation. *Geothermics*, 40(3):199–210.

Nick, H., Paluszny, A., Blunt, M., and Matthai, S. (2011). Role of geomechanically grown fractures on dispersive transport in heterogeneous geological formations. *Physical Review E*, 84(5):056301.

Nick, H., Schotting, R., Gutierrez-Neri, M., and Johannsen, K. (2009). Modeling transverse dispersion and variable density flow in porous media. *Transport in porous media*, 78(1):11–35.

Poulsen, S., Balling, N., and Nielsen, S. (2015). A parametric study of the thermal recharge of low enthalpy geothermal reservoirs. *Geothermics*, 53(0):464 – 478.

Pranter, M. J., Ellison, A. I., Cole, R. D., and Patterson, P. E. (2007). Analysis and modeling of intermediate-scale reservoir heterogeneity based on a fluvial point-bar outcrop analog, williams fork formation, piceance basin, colorado. *AAPG bulletin*, 91(7):1025–1051.

Saeid, S., Al-Khoury, R., Nick, H. M., and Barends, F. (2014). Experimentalânumerical study of heat flow in deep low-enthalpy geothermal conditions. *Renewable Energy*, 62(0):716 – 730.

Saeid, S., Al-Khoury, R., Nick, H. M., and Hicks, M. A. (2015). A prototype design model for deep low-enthalpy hydrothermal systems. *Renewable Energy*, 77(0):408 – 422.

Scheidegger, A. (1961). General theory of dispersion in porous media. *Journal of Geophysical Research*, 66(10):3273–3278.

TNO (1977). Nl olie- en gasportaal, www.nlog.nl.

van Heekeren, V., editor (2015). *The Netherlands country update on geothermal energy*, Stichting Platform Geothermie. World Geothermal Congress.

Willis, B. J. and Tang, H. (2010). Three-dimensional connectivity of point-bar deposits. *Journal of Sedimentary Research*, 80(5):440–454.